# Electrochemical Desorption and Adsorption of Nonyl Mercaptan at Gold Single Crystal Electrode Surfaces

**ARTICLE** *in* LANGMUIR · DECEMBER 1996

Impact Factor: 4.46 · DOI: 10.1021/la960365q



**3 AUTHORS**, INCLUDING:

Dongfang Yang
National Research Council Canada
**64** PUBLICATIONS **1,319** CITATIONS

SEE PROFILE

Mario Morin
Université du Québec à Montréal
**52** PUBLICATIONS **1,614** CITATIONS

SEE PROFILE

# Electrochemical Desorption and Adsorption of Nonyl Mercaptan at Gold Single Crystal Electrode Surfaces

D.-F. Yang,† C. P. Wilde,‡ and M. Morin*,†

*Ottawa−Carleton Chemistry Institute and Department of Chemistry, University of Ottawa, Ottawa, Ontario, Canada K1N 6N5, and Department of Chemistry, Imperial College of Science, Technology and Medicine, London SW7 2AY, U.K.*

*Received April 15, 1996. In Final Form: October 2, 1996*⊗

The electrochemical behavior of a nonanethiol layer adsorbed on Au(111), Au(110), and on a Au polycrystal has been examined using cyclic voltammetry. The reductive desorption and the oxidative redeposition of the nonanethiol molecules at the Au(111) surface have been shown to depend strongly on the pH of the electrolyte solutions. While the amount of material reductively desorbed from the surface on the first cathodic cycle is independent of the pH, the amount of material that is oxidatively redeposited increases significantly as the pH is lowered. This behavior is ascribed to a reduction in solubility of the product of desorption (thiolate or thiol) as pH decreases. At high pH the redeposition of the layer seems to occur in one step, but at pH values that are lower than the p$K_a$ of the nonanethiol the redeposition seems to occur in two steps. In an alkaline solution, the reductive desorption of the nonanethiols from a Au(110) surface is similar to the same process at the Au(111) surface. The double layer charging current, the shape of the reductive current peak, and its integrated charge are similar to those measured on the Au(111) electrode. Our single crystals study also reveals a correlation between the potential of zero charge of the uncoated gold single crystal electrodes and the potential at which the reductive desorption of the nonanethiols occurs. The results on a polycrystalline surface indicate a complex stripping pattern that is related to the different crystallographic domains present on the polycrystalline electrode.

## Introduction

Chemisorbed, self-organized, organic films on solid surfaces are a promising new class of materials with a wide range of applications.[1,2] The order of such films is critical for many potential uses of these films such as corrosion inhibitors or as optical materials; however, the conditions under which an ordered film is formed and maintained are not completely understood. For the class of self-assembled monolayers formed by alkanethiols on gold surfaces, the initial stage of film formation involves the fast adsorption of a thiol on the gold surface,[3−5] but the process of self-assembly is believed to be slow because it requires the migration of gold atoms from defect sites to more ordered terraces.[3,4,6−8] To understand better how self-assembly can occur and be maintained, it is important to understand both the gold−sulfur interactions as well as the interactions between neighboring alkane chains. Electrochemical studies allow the strength of chemical bonds of molecules adsorbed on electrode surfaces to be found[9] and information on the compactness of the organic layer can be obtained from permeation experiments.[10] Furthermore, the development of well-established methods for the preparation and use of single crystal electrodes in the study of electrochemical reactions[11] means that the effects of the crystallographic orientation on the rate of reaction occurring at the liquid/solid interface can be studied.

The structure of thiol self-assembled monolayers has been studied extensively using a variety of probes and single-crystal gold surfaces as substrates. He diffraction and grazing incidence X-ray diffraction (GIDX) experiments have shown that different ordered structures of the organic monolayer are formed and that the sulfur adsorbs on different sites on different gold single crystal surface orientations.[12] On the most studied Au(111) surface a variety of ($m\sqrt{3}\times n\sqrt{3}$)$R$30°) structures have been observed[8,12−15] whereas on the Au(110) surface the thiol monolayer forms a c(2 × 2) structure.[12] It was suggested that the sulfur adsorbs on a 3-fold site on the Au(111), but more recent studies suggest the presence of two types of sulfur which would be adsorbed on different sites.[15,16] On the Au(110) surface the thiols would adsorb on a 4-fold adsorption site.[12]

Numerous electrochemical studies of the ion permeation of thiol self-assembled monolayers, of the reduction and oxidation processes of derivatized thiols, and of the reductive and the oxidative removals of thiols have been reported.[10,17−26] However, in these studies the gold substrate was either a gold polycrystal or a gold film. The

* Corresponding author: e-mail, mgmorin@oreo.chem.uottawa.ca.
† University of Ottawa.
‡ Imperial College of Science, Technology and Medicine.
⊗ Abstract published in *Advance ACS Abstracts,* December 1, 1996.

(1) Ulman, A. *An introduction to ultrathin organic films: From Langmuir Blodgett to Self Assembly*; Academic Press: Boston, 1991.
(2) Kumar, A.; Abbott, N. L.; Kim, E.; Biebuyck, H. A.; Whitesides, G. M. *Acc. Chem. Res.* **1995**, *28*, 219.
(3) Buck, M.; Eisert, F. *J. Electron Spectrosc. Rel. Phenom.* **1993**, *64/65*, 159.
(4) Hahner, G.; Woll, Ch.; Buck, M.; Grunze, M. *Langmuir* **1993**, *9*, 1955.
(5) Karpovich, D. S.; Blanchard, G. J. *Langmuir* **1994**, *10*, 3315.
(6) Edinger, K.; Golzhauser, A.; Demota, K.; Woll, Ch.; Grunze, M. *Langmuir* **1993**, *9*, 4
(7) McCarley, R. L.; Dunaway, D. J.; Willicut, R. J. *Langmuir* **1993**, *9*, 2775.
(8) Poirier, G. E.; Tarlov, M. J. *Langmuir* **1994**, *10*, 2853.
(9) Bard, A. J.; Faulkner, R. J. *Electrochemical methods: Fundamentals and applications*; Wiley: New York, 1980.
(10) Porter, M. D.; Bright, T. B.; Allara, D. L.; Chidsey, C. E. D. *J. Am. Chem. Soc.* **1987**, *109*, 3559.
(11) Hamelin, A.; Vitanov, T.; Sevastyanov, E.; Popov, A. *J. Electroanal. Chem.* **1983**, *145*, 225.
(12) Camillone, N., III; Chidsey, C. E. D.; Eisenberger, P.; Fenter, P.; Li, J.; Liang, K. S.; Liu, G.-Y.; Scoles, G. *J. Chem. Phys.* **1993**, *99*, 744.
(13) Camillone, N., III; Leung, T. Y. B.; Schwartz, P.; Eisenberger, P.; Scoles G. *Langmuir* **1996**, *12*, 2737.
(14) Camillone, N., III; Chidsey, C. E. D.; Liu, G. Y.; Scoles, G. *J. Chem. Phys.* **1993**, *98*, 4234.
(15) Fenter, P.; Eberhardt, A.; Eisenberger, P. *Science* **1994**, *266*, 1216.
(16) Zubragel, Ch.; Deuper, C.; Schneider, F.; Neumann, M.; Grunze, M.; Schertel, A.; Woll, Ch. *Chem. Phys. Lett.* **1995**, *238*, 308.
(17) Sondag-Huethorst, J. A. M.; Fokkink, L. G. J. *J. Electroanal. Chem.* **1994**, *367*, 49.
(18) Sondag-Huethorst, J. A. M.; Fokkink, L. G. J. *Langmuir* **1992**, *8*, 2560.

S0743-7463(96)00365-4 CCC: $12.00 

potential at which the thiol layer is reduced depends on the substrate. Thiols deposited on polycrystalline gold are reductively removed at more negative potential than when they are deposited on highly ordered (i.e., mainly Au(111) domains) gold films.[18] A recent electrochemical study[25] using gold deposited on various substrates suggests that the different voltammetric peaks observed during the reductive removal of a thiol layer are related to the adsorption of the thiol on different crystallographic domains present on the deposited gold films. The substrate also influences the electrochemical stability of the thiol layer in the double layer region. In-situ vibrational studies have revealed that thiols deposited on a rough gold substrate underwent spectral changes[27] whereas thiols deposited on a smooth gold substrate did not show any spectral changes.[28−30] The potential applied to a thiol-coated gold film also modifies its wetting properties, and this effect has been used to design gates to control the flow of a liquid and liquid lenses.[31−33]

In this study, we have examined the role of the gold substrate on the electrochemistry of a nonanethiol monolayer by using clean, well-defined, gold single crystals and also polycrystalline gold. We have chosen the nonanethiol because the electrochemical behavior of thiols of less than 10 carbons has not been characterized as well as that of the longer chain thiols. A short chain thiol will reveal the substrate differences more easily than a longer chain thiol which blocks the ion transfer so efficiently that small electrochemical differences between substrates might be masked. Also the electrochemistry of the chemisorbed nonanethiol probed by cyclic voltammetry might differ from that of smaller, soluble, thiols and that of larger, insoluble, thiols. The effects of pH and potential scan rates have been employed to probe the reductive desorption and the oxidative redeposition of the nonanethiols on a Au(111) single crystal electrode. Finally, voltammetry at high pH for Au(110) and a polycrystalline gold electrode allows the effect of crystal orientation on the reductive desorption and oxidative redeposition processes to be evaluated.

## Experimental Section

Cyclic voltammetry experiments were performed in a three-electrode cell. The working electrode was a Au(111) or Au(110) single crystal or a polycrystalline gold bead. The counter electrode was a gold foil, and the reference electrode was a saturated calomel electrode (SCE). The reference electrode was housed externally in a glass bottle which contained a saturated KCl solution and was connected to the electrolyte solution through a salt bridge. The solution in the cell was deaerated with argon prior to the voltammetric measurements. A three-electrode potentiostat was used to control the electrode potential. All the potential values given in this paper are relative to a saturated calomel electrode (SCE). All solutions were made from distilled water purified through a Milli-Q water system (>18 MΩ) (Milli-Q Plus, Millipore Corp.). The $KClO_4$ (Aldrich) was recrystallized twice from Milli-Q water. Suprapure KOH solution (99.995%, Alfa) and $HClO_4$ solution (70%, Seastar Chemicals Inc.) were used to adjust the pH of the solution. The nonanethiol was purchased from Aldrich. Its purity was checked by mass spectrometry, and no disulfide or thiol other than nonanethiol was detected.

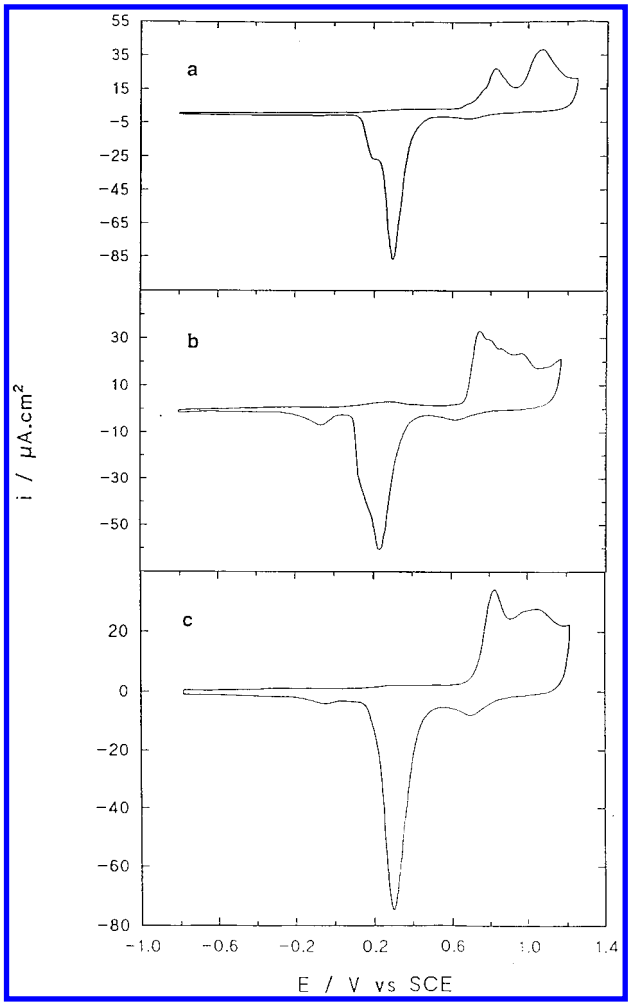


**Figure 1.** Cyclic voltammograms of (a) a Au(111) single crystal electrode; (b) a Au(110) single crystal electrode; (c) a gold polycrystal in a solution of 0.1 M $KClO_4$ at a potential scan rate of 20 mV $s^{-1}$.

The Au(111) and Au(110) single crystals were aligned to 0.1° using Laue X-ray back reflection. They were mechanically polished down to 0.01 $\mu$m with alumina paste and then electrochemically polished in perchloric acid. The approximate geometric area of the Au(111) electrode is 0.08 $cm^2$ and for the Au(110) the geometric area is 0.25 $cm^2$. The single crystals were then cleaned by repetitive oxidation−reduction cycles between −0.2 and 1.2 V in a 0.1 M $HClO_4$ solution. The Au(111) and Au(110) were flame-annealed[34] in a natural gas flame and cooled partially in air and quenched with deionized water and then immersed in the electrolyte solution under potential control. The quality and cleanliness of the single crystals were judged by recording a cyclic voltammogram in 0.1 M $KClO_4$ using the hanging meniscus technique where the electrode is pulled up to form a meniscus so that only the single crystal surface is in contact with the solution. Parts a and b of Figure 1 show the resulting cyclic voltammograms for the clean Au(111) and Au(110) electrodes, respectively. The voltammograms are identical to

(19) Sondag-Huethorst, J. A. M.; Fokkink, L. G. J. *Langmuir* **1995**, *11*, 2237.
(20) Finklea, H. O.; Avery, S.; Lynch, M.; Furtsch, T. *Langmuir* **1987**, *3*, 409.
(21) Bunding-Lee, K. A.; Mowry, R.; McLennan; Finklea, H. O. *J. Electroanal. Chem.* **1988**, *246*, 217.
(22) Sabatini, E.; Rubinstein, I.; Maoz, R.; Sagiv, J. *J. Electroanal. Chem.* **1987**, *219*, 365.
(23) Sato, Y.; Ye, S.; Haba, T.; Uosaki, K. *Langmuir* **1996**, *12*, 2726.
(24) Weisshaar, D. E.; Lamp, B. D.; Porter, M. D. *J. Am. Chem. Soc.* **1992**, *114*, 5860.
(25) Walczak, M. M.; Aves, C. A.; Lamp, B. D.; Porter, M. D. *J. Electroanal. Chem.* **1995**, *396*, 103.
(26) Widrig, C. A.; Chung, C.; Porter, M. D. *J. Electroanal. Chem.* **1991**, *310*, 335.
(27) Anderson, M. R.; Gatin, M. *Langmuir* **1994**, *10*, 1638.
(28) Popenoe, D. D.; Deinhammer, R. S.; Porter, M. D. *Langmuir* **1992**, *8*, 2521.
(29) Hines, M. A.; Todd, J. A.; Guyot-Sionnest, P. *Langmuir* **1995**, *11*, 493.
(30) Yang, D.-F.; Al-Maznai, H.; Morin, M. *J. Phys. Chem.*, in press.
(31) Abbott, N. L.; Whitesides, G. M. *Langmuir* **1994**, *10*, 1493.
(32) Abbott, N. L.; Gorman, C. B.; Whitesides, G. M. *Langmuir* **1995**, *11*, 16.
(33) Gorman, C. B.; Biebuyck, H. A.; Whitesides, G. M. *Langmuir* **1995**, *11*, 2242.
(34) Clavilier, J.; Faure, R.; Guinet, G.; Durand, R. *J. Electroanal. Chem.* **1980**, *107*, 205.

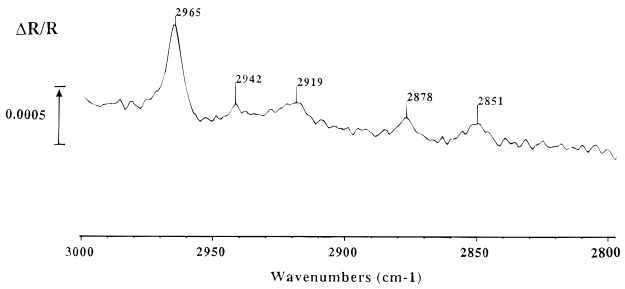


**Figure 2.** Infrared reflection−absorption spectrum of a nonanethiol layer chemisorbed on a Au(111) electrode. The spectrum was taken at a resolution of 2 $cm^{-1}$ with p-polarized light and is an average of 1000 scans.

those reported in the literature.[35,36] The polycrystalline gold electrode was made by melting one end of a gold wire (99.9985%, 1 mm in diameter, Alfa) in a natural gas−air flame to form a drop. The drop was cooled down slowly in air. The resulting gold bead consisted of a few crystalline domains as shown by etching in warm aqua regia. The polycrystalline gold was electrochemically cleaned using the same procedure as described above. Figure 1c shows the voltammogram for the immersed polycrystalline electrode recorded in the 0.1 M $KClO_4$ solution. It is also similar to previous results.[37]

The clean gold electrodes were immersed in a nonanethiol solution ($10^{-2}$ M in ethanol (Denatured, BDH)) for a period of 30 min to form a monolayer of the thiol on the electrode surface. After the electrode was emersed from the thiol solution, it was rinsed thoroughly with ethanol and then with Milli-Q water and then was transferred (under potential control) to the electrochemical cell containing the pure supporting electrolyte and a hanging meniscus was formed. In all the experiments presented here, the potential of the electrode is initially scanned to the negative (i.e., cathodic) potential region and then scanned in the reverse direction (i.e., in the positive potential direction). The resulting cyclic voltammograms were recorded as a function of the number of scans, the potential scan rate, and the pH of the electrolyte solution.

## Results and Discussion

The quality of the nonanethiol layer was checked by infrared reflection−absorption spectroscopy. The ex-situ infrared spectrum of the CH stretching region is shown in Figure 2. The methyl CH stretching bands are at 2965, 2942, and 2878 $cm^{-1}$ and the methylene bands are at 2919 and 2851 $cm^{-1}$. The assignment of these bands is the same as previously reported.[38,39] The frequencies of the bands and their relative intensities are in agreement with a previous study of short chain thiols and indicative of an aliphatic chain in an all-trans configuration.[40] More specifically the large intensity of the methyl mode at 2965 $cm^{-1}$ is in agreement with previous studies of aliphatic thiols with an odd number of carbons.[41] The CH stretching modes at 2965, 2942, and 2878 $cm^{-1}$ of the terminal methyl group are narrow (~10 $cm^{-1}$ fwhm). We take these observations as indications that the sample preparation method used here yields a homogeneous monolayer.

The small double layer charging current of 50 nA $cm^{-2}$ (±10%) in a solution of 0.1 M KOH (Figure 3) illustrates that the nonanethiol forms a good blocking monolayer on the electrode surface. This value is independent of the

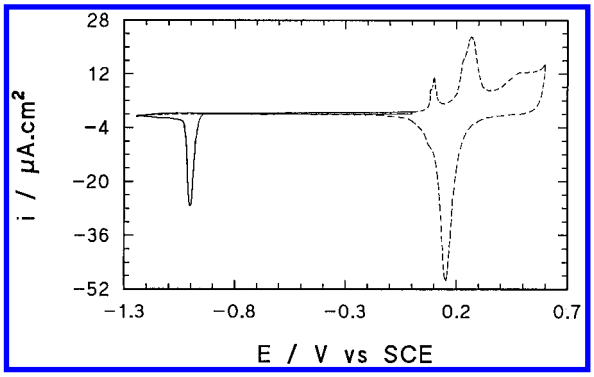


**Figure 3.** Cyclic voltammogram of a nonanethiol-coated Au(111) electrode in 0.1 M KOH at a potential scan rate of 10 mV $s^{-1}$: solid line, first cathodic scan; dashed line, first anodic scan and second cathodic scan.

electrolyte pH and varies linearly with the potential scan rate between 1 and 100 mV $s^{-1}$ (correlation factor of 0.998). The anodic and the cathodic currents recorded over the double layer region (ca. between −0.8 and 0.0 V) are constant and equal but opposite in sign. These measured voltammetric properties indicate that the nonanethiol-coated Au(111) electrode can be represented by a simple capacitor. The double layer capacitance of the nonanethiol-coated electrode can thus be estimated from the voltammetric data[9] and is found to be 2.5 $\mu$F $cm^{-2}$ (±10%). This value is similar to the capacitance value determined for the same molecule adsorbed on Au evaporated on mica.[26] Although these results are not as accurate as the differential capacitance measurements reported previously,[17−19] they do indicate that the nonanethiol layer is quite compact. The stability of the nonanethiol monolayer in the double layer region is supported by the absence of spectral changes between 0.10 and −0.95 V in the in-situ vibrational spectra of the nonanethiol monolayer.[30] The voltammetric results combined with the in-situ and ex-situ infrared spectra of the nonanethiol chemisorbed on the Au(111) further show that the nonanethiols form a compact, homogeneous monolayer.

The main aspect of interest in this paper is the reductive desorption and subsequent oxidative redeposition of the thiols and the factors which influence this process. Successive cyclic voltammograms of a nonanethiol-coated Au(111) electrode between −1.20 and 0.6 V in 0.1 M KOH are shown in Figure 3. The coated electrode is first immersed in the electrolyte solution at a potential of 0.00 V. The potential is then scanned in the negative direction. The first feature that is seen (solid line) is a sharp, symmetric, reductive current peak at −1.04 V. The subsequent features of the voltammogram and the data in Figure 3 indicate that this peak is associated with a one-electron reductive desorption of the thiols and is not associated with a capacitative change. When the potential is reversed and scanned in the positive direction, no oxidative features are observed from −1.20 to 0.00 V, but the gold surface oxide formation begins to appear at potentials more positive than 0.00 V as shown by the dashed line. The gold oxide layer that is formed is identical to that of a clean Au(111) single crystal electrode in 0.1 M KOH. On the second cathodic (i.e., negative going) potential scan the only reduction peak that is observed is at 0.15 V and corresponds to reduction of the gold surface oxide. On the second anodic (i.e., positive going) potential scan only gold surface oxide formation is observed. The third cycle gives a voltammogram characteristic of an uncoated Au(111) surface in 0.1 M KOH.

These results clearly show that the thiols are removed from the surface. When chemisorbed nonanethiols are present on the surface, the current associated with the

(35) Stolberg, L.; Lipkowski, J.; Irish, D. E. *J. Electroanal. Chem.* **1990**, *296*, 171.
(36) Richer, J.; Lipkowski, J. *J. Electrochem. Soc.* **1986**, *133*, 121.
(37) Stolberg, L.; Richer, J.; Lipkowski, J.; Irish, D. E. *J. Electroanal. Chem.* **1986**, *207*, 213.
(38) Nuzzo, R. G.; Dubois, L. H.; Allara, D. L. *J. Am. Chem. Soc.* **1990**, *112*, 558.
(39) Porter, M. D.; Bright, T. B.; Allara, D. L.; Chidsey, C. E. D. *J. Am. Chem. Soc.* **1987**, *109*, 3559.
(40) Allara, D. L.; Nuzzo, R. G. *Langmuir* **1985**, *1*, 45.
(41) Dubois, L. H.; Zegarski, B. R.; Nuzzo, R. G. *J. Electron Spectrosc. Rel. Phenom.* **1990**, *54/55*, 1143.

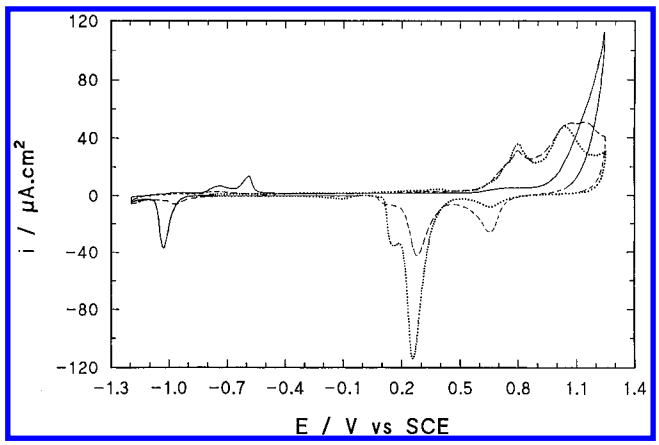


**Figure 4.** Cyclic voltammogram of a nonanethiol-coated Au(111) electrode in 0.1 M $KClO_4$ at a potential scan rate of 20 mV $s^{-1}$: solid line, first cycle; dashed line, second cycle; dotted line, third cycle.

gold oxide formation at a scan rate of 10 mV/s is considerably attenuated. Figure 3 does not show this effect, and since at the start of the cycle at 0.0 V the electrode is covered with a monolayer of thiol, the gold−sulfur bonds must be broken in the reductive process seen at −1.04 V. We therefore assign the reductive current peak at −1.04 V to charge transfer from the electrode to the thiols. In-situ infrared measurements that will be presented elsewhere[30] support this interpretation. Large spectral changes in the CH stretching bands are seen when the electrode potential is stepped from −0.50 to −1.10 V just past the reductive current peak. It should be noted that the reductive current peak has two components.[25,42] The most important component is the charge transfer between the electrode and the chemisorbed thiols but there is also a smaller capacitive component linked to the formation of the double layer on the uncoated gold electrode after thiol removal. This is estimated below.

When reductive desorption of the thiol is performed in electrolytes of lower pH, new oxidation peaks are observed after the reductive desorption, and these can be shown to be the result of oxidative redeposition of the thiols. Figure 4 shows an equivalent experiment to Figure 3 for a nonanethiol-coated Au(111) electrode in 0.1 M $KClO_4$. The voltammogram differs significantly from that in Figure 3. On the first cathodic potential scan (solid line) a large reductive current peak is seen at −1.00 V. The integrated charge obtained from this reductive current peak is identical (±10%) to that obtained from the data in Figure 3, and this feature is again assigned to reductive desorption of the thiol. The new features are then seen on the first anodic potential scan and are the two large oxidative current peaks at −0.72 and −0.60 V. There is then no more oxidative electrochemistry until the formation of the gold surface oxide is seen at the upper potential limit. The amount of gold surface oxide formed is considerably smaller than the amount formed at an uncoated Au(111) electrode (see Figure 1a), and the onset of the oxide formation is at a more positive potential. On the second cathodic potential scan (dashed line), peaks corresponding to gold oxide reduction are seen at 0.67 and 0.28 V followed by a large region where no Faradaic electrochemistry occurs until the small reductive peak at −0.97 V. This peak is smaller than the one observed on the first cathodic scan. On the second anodic potential scan we still see a broad oxidative current between −0.8 and −0.7 V but it is smaller than the one observed on the first anodic potential scan. Finally, a more substantial gold surface oxide formation is observed beginning at 0.6 V, significantly earlier than the gold oxidation current of the first cycle. After three cycles (dotted line) a voltammogram similar to that of an uncoated Au(111) electrode in 0.1 M $KClO_4$ is obtained. All the thiols are removed from the surface after four voltammetric cycles since a voltammogram identical to that in Figure 1a is then observed.

The successive voltammograms in Figure 4 establish a correlation between the reductive and the oxidative current peaks observed between −1.20 and −0.60 V (in fact the only peaks observed below 0.0V) and the amount of gold surface oxide that is formed (the peaks observed at potentials greater than 0.0V). As the reductive peak at ca. −1.0 V decreases, the amount of gold oxide formed increases. These results show that fewer and fewer thiols are chemisorbed on the surface as the number of voltammetric cycles increases. They also show that the reductive peak at ca. −1.0 V is mainly due to the Faradaic current caused by the reductive desorption of the thiols and is not purely capacitive. The oxidative current peaks at −0.72 and −0.60 V observed in 0.1 M $KClO_4$ (Figure 4) can be attributed to oxidative redeposition of the reductively desorbed molecules. Several facts support this assertion. First, the disappearance of these oxidative redeposition peaks corresponds to the appearance of increased gold surface oxidation, and when no oxidative peaks are seen, as in the third or fourth cycle in 0.1 M $KClO_4$ or as in 0.1 M KOH, a complete gold oxide layer is formed. These peaks are therefore linked to the presence of adsorbed molecules that block the formation of the gold surface oxide. Second, the oxidative current peaks between −0.8 and −0.5 V are related to the reductive current peak seen at −1.0 V. The integrated charge of these oxidative current peaks (Figure 4) is always less than the integrated charge of the reductive current peak on the previous cathodic scan. Third, when the positive potential limit is set at 0.0 V, where no gold surface oxide is formed, the integrated charge of the oxidative current peaks is equal (±5%) to the integrated charge of the reductive current peak on the subsequent cathodic scan. These observations strongly suggest that the oxidative current peak is associated with the oxidative readsorption of the reductively desorbed molecules. The charge and voltammetric data show that the reductive removal of the thiol is complete but that the redeposition is not and so repeated cycling results in slow removal of the monolayer. These observations also show that the oxidative current peaks at −0.72 and −0.60 V are not purely capacitive in nature.

The voltammetric results in Figures 3 and 4 clearly show that the pH of the electrolyte solution influences both the reductive desorption and the oxidative redeposition of the thiols. The changes in the cyclic voltammograms as a function of the pH of the electrolyte solution have been investigated further. The first cathodic potential scans as a function of the pH are shown in Figure 5. The collected data may be divided into three sets spanning the pH ranges from 13 to 10.5, 10.5 to about 7, and then the region below 7. First, in the pH range from 13 to 10.5 the reductive process is not influenced greatly by the pH since only one relatively sharp (ca. 40 mV fwhm) reductive peak is observed at −1.04 V. However, pH 10.5 marks the beginning of a transition region. The reductive current peak broadens from 40 to 55 mV fwhm as the pH decreases from 13 to 10.5. When the pH is further decreased from 13 to 7 the reductive current peak is only shifted by 40 mV to −1.00 V. However, at a pH of 7 the reductive current continues to broaden (60 mV fwhm). When the pH is decreased to 5.9, a small peak becomes visible at −0.78 V in addition to the main reductive current

(42) Lipkowski, J. In *Modern Aspects of Electrochemistry*; Conway, B. E., Bockris, J. O'M., White, R. E., Eds.; Plenum: New York, 1992; Vol. 23, Chapter 1.

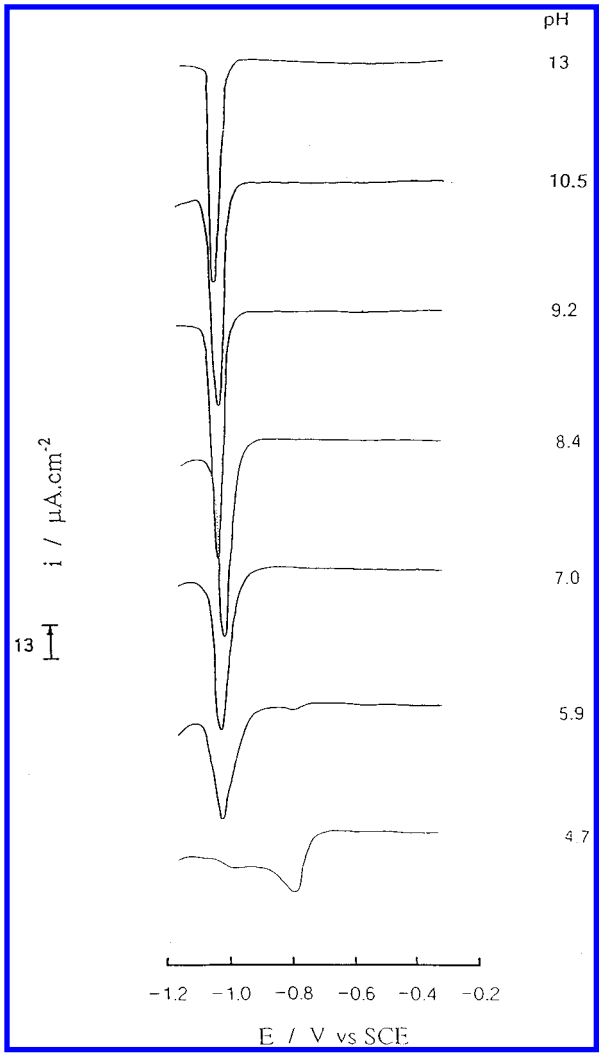


**Figure 5.** First cathodic cycle of a nonanethiol-coated Au(111) electrode in solutions of different pH at a potential scan rate of 20 mV/s.

peak which is now considerably broadened. This former peak becomes predominant at pH 4.7, while the reductive current peak at −1.00 V diminishes noticeably. In addition, a significant reduction current due to hydrogen evolution is seen at a pH of 4.7.

Despite the changes in the shape and the potential location of the reductive current peaks noted above, the integration of the reductive desorption peak at every pH (except at 4.7 because of the significant hydrogen evolution) gives the same charge of 100 $\mu$C cm$^{-2}$ (±10%). In a 0.1 M KOH solution, this integrated reductive charge is found to be independent (±10%) of the potential scan rate between 1 and 120 mV s$^{-1}$. Thus the charge required for complete reductive desorption of the thiol monolayer is constant over a variation of 2 orders of magnitude in the potential scan rate. This behavior is typical of a fast charge transfer between an electrode and a chemisorbed species.[9] Under the same experimental conditions, the reductive charge associated with the removal of an hexadecanethiol layer[43] is found to be 100 $\mu$C cm$^{-2}$ (±10%). This value is, within the uncertainties of the measurements, identical to that of a nonanethiol monolayer. Our calculated reductive charge is similar to the value reported by Widrig et al.[26] for reductive desorption of *n*-alkanethiols of different chain lengths at an Au/mica electrode (90 ± 7 $\mu$C cm$^{-2}$). We therefore believe that the calculated charge is representative of the reductive desorption of the thiols.

(43) Yang, D.-F.; Wilde, C. P.; Morin, M. *Langmuir*, in press.

Given the assertion above, the thiol coverage can be obtained from the integrated reductive charge. As mentioned before, the charge associated with the desorption of a monolayer of nonanethiol consists of capacitive and Faradaic contributions. The thiol coverage is estimated from the latter, and so the former contribution must be subtracted from the total integrated reductive charge. The capacitive charge, $\Delta Q$, results from the difference between the double layer charge of the coated electrode, $Q_1$, and the double layer charge of the uncoated Au(111) electrode, $Q_2$. The capacitive charge, $\Delta Q$, can be crudely estimated as follows: We assume that the coated electrode is a perfect capacitor. The charge, $Q_1$, accumulated by a capacitor is calculated from the following equation: $Q_1 = C_1(E_1 - E_{1,pzc})$, where $C_1$ is the electrode capacitance at a potential $E_1$. $E_{1,pzc}$ is the potential of zero charge of the coated single crystal electrode. The uncoated electrode is not a perfect capacitor[44] and the double layer charge is obtained from chronocoulometric measurements.[45]

As an example, we analyze the data obtained in a 0.1 M KOH solution since the current assigned to the reductive removal of the thiols is well separated from the hydrogen evolution current and the nonanethiol monolayer is completely removed in a single cathodic potential scan. The double layer charge of the uncoated electrode, $Q_2$, at a potential of −1.1 V is −32 $\mu$C cm$^{-2}$.[45] The exact evaluation of the double layer charge, $Q_1$, of the nonanethiol-coated Au(111) electrode is not possible because $E_{1,pzc}$ is not known. Nevertheless, an estimation of $\Delta Q$ can be made since the charging of the double layer of the uncoated Au(111) electrode requires a charge $Q_2$ that is much larger than $Q_1$ because of the low double layer capacitance of the coated electrode. To estimate $Q_1$, we assume that $E_{1,pzc}$ is located between −0.45 V, which is the maximum of the electrocapillary curve of a thiol-coated polycrystalline electrode,[17] and the pzc of the uncoated Au(111) electrode of 0.28 V. $E_1$ is taken to be −0.9 V just before the reductive current peak. For this large variation of $E_{1,pzc}$, $Q_1$ only changes from −1 to −3 $\mu$C cm$^{-2}$ and $\Delta Q$ from 31 to 29 $\mu$C cm$^{-2}$. Thus the error in the estimation of the capacitive charge is smaller than the uncertainties in our measurements of the total reductive charge. The magnitude of the capacitive charge is similar to the values reported for the desorption of Langmuir−Blodgett films of octadecanol (~25 $\mu$C cm$^{-2}$) from a Au(111) electrode.[46,47] It is clear from these results on Au(111) single crystal electrodes that a total reductive charge of 100 $\mu$C cm$^{-2}$ is too large to be due to a capacitive process alone.

Subtraction of the capacitive contribution from the total charge gives a calculated Faradaic charge of between 69 and 71 $\mu$C cm$^{-2}$ associated with the reductive desorption of the thiols. About a quarter of the total reductive charge is due to the change in the double-layer capacitance as the surface is transformed from thiol-coated to clean gold. The thiol surface coverage is then calculated by assuming that the reduction of one molecule of nonanethiol requires one electron. The one-electron mechanism is supported by in-situ infrared data of the reductive desorption of the nonanethiols that shows that the desorbed species in 0.1 M KOH is a thiolate.[30] The thiol surface concentration is found to be between 7.1 and 7.3 × 10$^{-10}$ mol cm$^{-2}$ (±10%) giving a ratio of one nonanethiol per three surface gold atoms. The results of helium diffraction and GIXD,[12−15]

(44) Hamelin, A. In *Modern Aspects of Electrochemistry*; Conway, B. E., White, R. E., Bockris, J. O'M., Eds.; Plenum: New York, 1985; Vol. 16, Chapter 1.
(45) Yang, D.-F.; Lipkowski, J. *Langmuir* **1994**, *10*, 2647.
(46) Bizzotto, D.; Noel, J. J.; Lipkowski, J. *J. Electroanal. Chem.* **1994**, *369*, 259.
(47) Bizzotto, D.; Lipkowski, J. *Prog. Surf. Sci.* **1995**, *50*, 237.

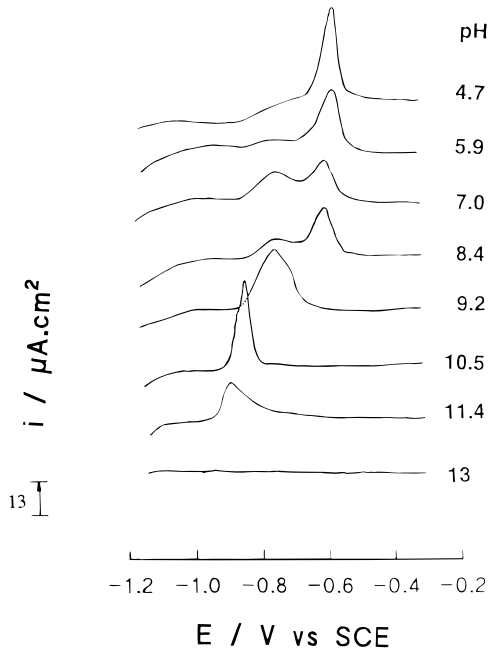


**Figure 6.** First anodic cycle of a nonanethiol-coated Au(111) electrode in solutions of different pH at a potential scan rate of 20 mV $s^{-1}$.

electron diffraction,[48] and scanning tunneling microscopy[8] studies show that alkanethiols form a $(\sqrt{3}\times\sqrt{3})R30°$ overlayer on the Au(111) surface. A perfect overlayer structure would give a coverage of $7.6 \times 10^{-10}$ mol $cm^{-2}$. Even considering the uncertainties in the models used to obtain the surface coverage of the thiol from the voltammetric data, it is clear that a high-coverage, compact, nonanethiol layer can be formed on the Au(111) surface using the sample preparation methods employed in this study.

As noted above, there is a pH dependence of both the reductive desorption and the oxidative redeposition of the thiol, and the most striking observations in this study are shown in Figure 6. A strong pH dependence of the oxidative redeposition peaks on the first anodic scan is revealed. At a pH of 13 and a scan rate of 20 mV $s^{-1}$ there is no oxidative current peak. Hence, no desorbed molecules are oxidatively redeposited. At 120 mV $s^{-1}$ (data not shown), a small oxidative peak is seen. Thus the redeposition of thiols is kinetically limited. When the pH is lowered to 11.4, a small oxidative current peak appears at −0.92 V and further decreases of pH lead to more changes in the redeposition process. At pH 10.5 the oxidative current peak becomes larger and sharper and moves to −0.88 V and a small shoulder appears on the negative potential side of the main peak. The charge under the oxidative peak is now 50% (±10%) of the integrated charge of the reductive peak seen on the previous cathodic scan. More significant changes are seen at pH 9.2, where the oxidative current peak broadens and its potential is shifted by +100 mV to −0.78 V. A shoulder also appears on the positive side of the main current peak. The charge of the oxidative redeposition peak is now about 80% (±10%) of the reductive charge seen on the previous cathodic potential scan. Interestingly the large potential shift of +100 mV of the oxidative current peak at pH 9.2 occurs at a pH close to the p$K_a$ of nonanethiols in aqueous solution,[49] which is estimated to be around 10. For solutions of pH between 8.4 and 4.7, two well-separated oxidative current peaks are observed. At a pH of 8.4, one oxidative current peak is located at −0.78 V and is broad, while the other peak is at −0.61 V and is sharper. As the pH decreases from 8.4 to 4.7 the current peak at the more negative potential becomes smaller and the current peak at the more positive potential becomes larger.

The increase of the oxidative current peak as the pH of the electrolyte solution decreases for the slow scan rate of 20 mV $s^{-1}$ means that the extent of oxidatively redeposited material increases as the pH decreases. This result is surprising if we consider that there is at least 15 s between the reductive desorption and the oxidative redeposition at the slow potential scan rate of 20 mV $s^{-1}$. We should not expect that up to 80% of the desorbed molecules in 0.1 M $KClO_4$ will be redeposited. We can only suggest at this stage that the extent of redeposition is linked to the solubility of the desorbed thiolates. It is known[50] that up to 2.3 g $L^{-1}$ of nonanethiol can be dissolved in 1 M NaOH and only 1.15 mg $L^{-1}$ can be dissolved in water. This large change in solubility is due to the fact that at a pH of 14 the nonanethiol is unprotonated since it has a p$K_a$ of ∼10.[49] The ionic nonanethiolate is more soluble in water than the neutral nonanethiol. The variation by 3 orders of magnitude of the solubility of the nonanethiol with a variation of 7 pH units will most certainly play a role in the observed increase in the oxidative current peak. Furthermore, the repulsive interactions between the nonanethiolates will not favor their redeposition. It is noticeable that the most significant changes in both the voltammograms for the reductive desorption and for the oxidative redeposition occur in the pH range of 8 to 10, which is close to the p$K_a$ of a nonanethiol. This further suggests that the protonation of the thiols plays a role in the oxidative redeposition of the nonanethiols.

The significant oxidative redeposition of reductively desorbed thiols is not limited to the nonanethiols. For a hexadecanethiol monolayer deposited on a Au(111) single crystal the integrated charge of the oxidative peak seen after the first reductive removal of the thiol is ∼90% (±5%) of the integrated charge of the reductive peak[43] in the pH range between 13 and 6 (potential scan rate = 20 mV $s^{-1}$). In contrast, for a butanethiol layer in 0.1 M $KClO_4$, the integrated charge of the oxidative current peak is only 20% (±10%) of the integrated charge of the previous reductive current peak (potential scan rate = 20 mV $s^{-1}$). The solubility of the butanethiol in alkaline and neutral aqueous solution does not vary as significantly as that of the nonanethiol. Butanethiol is soluble in 1 M NaOH, and 0.56 g $L^{-1}$ can be dissolved in water.[50] These results suggest a general trend in which the extent of oxidative deposition (when considered at a constant scan rate of 20 mV $s^{-1}$) increases with increasing chain length because of the decreasing solubility of the thiolate (alkaline solutions) and of the thiol (neutral solutions). Nonanethiol represents an intermediate case between hexadecanethiol, which may be redeposited with high efficiency even in alkaline solutions, and butanethiol, which is too soluble for significant redeposition even in neutral solutions. The reversible adsorption/desorption reported here has precedents in the case of many insoluble surfactants physisorbed on a Au(111) single crystal electrode which also undergo repetitive desorption and adsorption when the potential is cycled at slow potential scan rates (i.e., 20 mV $s^{-1}$ or less).[46,47]

The oxidative redeposition occurs in a single peak at pH higher than ∼10 and in two peaks at lower pHs at a scan rate of 20 mV $s^{-1}$. A potential scan rate dependence

(48) Strong, L.; Whitesides, G. M. *Langmuir* **1988**, *4*, 546.
(49) Serjeant, E. P.; Dempsey, B. *Ionization constants of organic compounds in aqueous solutions*, IUPAC chemical data series, no. 23; Pergamon Press: Oxford, 1983.
(50) Reid, E. E. *Organic Chemistry of Divalent Sulfur*; Chemical Publishing Co. Inc.: New York, 1958; Vol. 1.

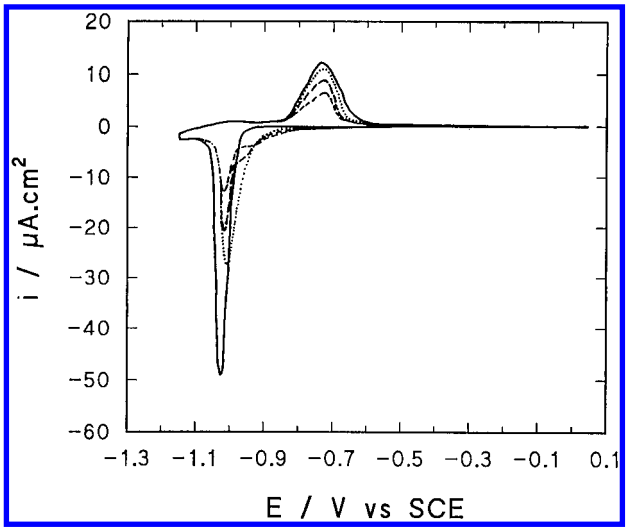


**Figure 7.** Consecutive cyclic voltammograms of a nonanethiol-coated Au(111) electrode in a solution of pH 9.2 at a potential scan rate of 20 mV $s^{-1}$. The first cycle is represented by the solid line, the second cycle is the dotted line and the fourth and sixth cycles are represented by the dashed lines.

from 5 to 120 mV $s^{-1}$ of the oxidative current peaks at a pH of 9.2 (data not shown) reveals that the two oxidative current peaks are kinetically different. The most positive oxidative peak represents the slower process since it moves to more negative potential when the scan rate is decreased, whereas the other current peak remains at the same potential. The fact that the onset of the voltammetric changes is at a pH of ca. 10, close to the p$K_a$ of the nonanethiol, suggests that the reprotonation of the thiols is involved in these changes.

Qualitative information on the state of the oxidatively redeposited layer is obtained from repetitive cycling experiments such as that shown in Figure 7. At a pH of 9.2, the oxidative peak decreases smoothly, the peak potential does not change and neither does the shape of the peak with increasing cycling. The reductive peak also decreases smoothly but shifts slightly to more positive potentials (∼10 mV) as it decreases in intensity, and a small current peak develops on the positive potential side of the peak as the total reductive current decreases. Another noticeable property of the nonanethiol layer is that the integrated charge of the oxidative peak is equal (±5%) to the integrated charge on the reductive current peak on the subsequent cathodic scan. This is a clear piece of evidence that the oxidative and reductive current peaks are correlated. Since the potentials at which the thiols are reductively desorbed and oxidatively redeposited do not vary significantly with the thiol surface coverage, then most of the oxidatively redeposited thiols are in an environment similar to that of the initial chemically deposited layer, even when coverage is much less than a monolayer. In-situ FTIR experiments are underway to probe the nature of these peaks.

Further insight into the state of the monolayer can be gained through the use of other single crystal orientations and through the use of a polycrystalline electrode. Beginning with the Au(110) single crystal, a monolayer-covered electrode was prepared according to the protocol described above for the Au(111) surface, and then the potential of the electrode was cycled from 0.1 to −1.35 V and back to 0.1 V. The initial stages of the scan reveal a double-layer charging current of 50 nA $cm^{-2}$ (±10%), a value identical to that measured on the Au(111) surface. Figure 8 shows that the reductive desorption (at 20 mV $s^{-1}$) of the nonanethiol from Au(110) in a solution of 0.1 M KOH gives a single, narrow peak at −1.27 V (solid line). The width of the reductive current peak is similar

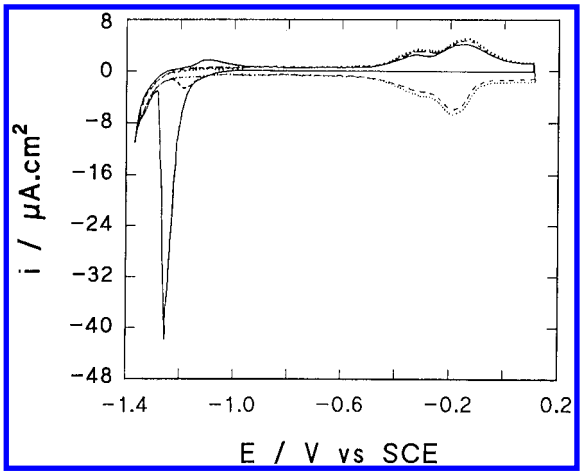


**Figure 8.** Cyclic voltammogram of a nonanethiol-coated Au-(110) electrode in 0.1 M KOH at a potential scan rate of 20 mV $s^{-1}$: solid line, first cycle; dashed line, second cycle; dotted line, third cycle.

(50 mV fwhm) to that of the peak observed on the Au(111) electrode. We therefore believe that on the Au(110) electrode the thiols form an ion blocking layer similar to that which is formed on the Au(111) surface. The onset of the reductive desorption of the nonanethiol on the Au-(110) surface is at −1.0 V and is not as sharp as the onset of reductive desorption from the Au(111) surface (see Figure 5). The difference between the reductive current peak potentials (230 mV) for the two single crystals is less than the difference in the potentials of zero charge (pzc) of ∼300 mV of the uncoated Au(111) and Au(110) surfaces.[51] There is a small oxidative current peak at −1.15 V on the subsequent anodic scan represented by the solid line. The oxidative current peaks between −0.5 and 0.1 V are due to the adsorption of hydroxyls. On the next cathodic scan (dashed line) the hydroxyls are reduced between 0.1 and −0.5 V and a small reduction peak at −1.2 V is seen. The third voltammetric cycle (dotted line) only shows the gold oxide formation and reduction.

The surface coverage of the nonanethiol on the Au(110) electrode was estimated using the same model as described above. The integration of the reductive peak on Au(110) gives a charge of 105 $\mu$C $cm^{-2}$ (±10%), a value which is almost identical to that obtained on the Au(111) surface. The capacitive charge was estimated from chronocoulometric measurements[37] and from our measurements of the double layer capacitance. The surface coverage of nonanethiol on Au(110) is $7.5 \times 10^{-10}$ mol $cm^{-2}$ (±10%), a value similar to the calculated value for the Au(111) surface. If the Au(110) surface is unreconstructed when monolayer formation occurs, as is often the case for anion adsorption,[52] the number of gold surface atoms on Au-(110) is smaller by a factor of ∼0.6 relative to the Au(111) surface. Therefore, on the Au(110) surface the ratio of the gold surface atoms to nonanethiol molecules is 2:1. This result is in good agreement with He diffraction[12] results which indicate that thiols adsorbed on the Au-(110) form a c(2 × 2) overlayer which has the same ratio of gold atoms to nonanethiol (2:1). These authors also suggest that the sulfur adsorbs at a 4-fold site. Although we cannot say that the positive 70 mV shift of the reductive current peak on the Au(110) (relative to what is expected from the pzc difference with the Au(111)) is only caused by a different adsorption site of the nonanethiol on the Au(111), we expect that it is an important factor. To

(51) Lipkowski, J.; Stolberg, L.; Yang, D.-F.; Pettinger, P.; Mirwald, M.; Henglein, F.; Kolb, D. M. *Electrochim. Acta* **1994**, *39*, 1045.
(52) Gao, X.; Weaver, M. J. *Surf. Sci.* **1994**, *313*, L775.

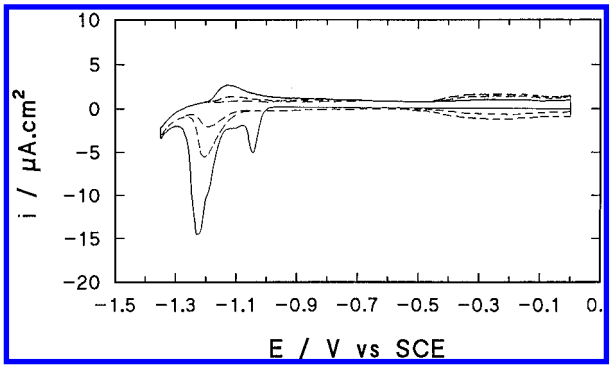


**Figure 9.** Cyclic voltammogram of a nonanethiol-coated gold polycrystalline electrode in 0.1 M KOH at a potential scan rate of 20 mV $s^{-1}$: solid line, first cycle; dashed line, second and third cycles.

evaluate the relative binding strengths of the thiols on the Au(111) and the Au(110) surfaces, we would need to know the potential of zero charge of the thiol-coated surfaces. These values are not known. The potential of zero charge depends on the interactions between the electrode and the adsorbates, the adsorbate coverage, the crystallographic orientation of the substrate, and possible surface reconstructions. It is therefore not possible to make an accurate prediction of the effect of thiol adsorption on the pzc. Nevertheless, our measurements indicate a correlation between the pzc of the clean electrode and the potential of the thiol reduction peak. We do not expect that the differences between the potential of the reductive current peaks on the Au(111) and Au(110) electrode are only caused by the differences in permeability of the nonanethiol layer on both surfaces since the double layer capacitances are very similar.

The reductive desorption and oxidative redeposition of the nonanethiol layer on a polycrystalline gold electrode gives further support to the role that the surface charge density and crystallographic orientation of the substrate play in the reductive desorption of the thiol molecule from the surface. On the polycrystal face (Figure 9), two main reductive current peaks are seen at potentials corresponding to the value measured on the Au(111) surface (−1.04 V, Figure 5) and close to the value measured for the Au(110) surface (−1.27 V, Figure 8) under the same conditions. These similarities suggest that the pzc values for different crystallographic orientations of the gold surfaces can be used to predict that the reductive removal of the nonanethiols will occur at a more negative potential on the smooth (100) face, stepped ((110) and (311)) faces, and kinked (210) faces than on the Au(111) face. This is due to the fact that the pzc for the Au(111) face is at 0.28 V, which is 140, 260, 300, and 380 mV more positive than the pzc values for the (100), (311), (110), and (210) faces, respectively.[51] The unresolved current peak at −1.14 V located 60 mV negative of the (111) peak is tentatively assigned to desorption from the (100) domains. Interestingly GIXD results[12] show that thiols adsorb on a 2-fold bridge site on Au(100), on a 3-fold site on the Au(111) surface, and on a 4-fold site on the Au(110). The dashed lines on Figure 9 represent the second and third voltammetric cycles. They show a rapid decrease of the reductive and oxidative current peaks between −0.9 and −1.4 V which are associated with the thiol reductive desorption and oxidative redeposition. The reductive and oxidative currents at potentials more positive than −0.5 V are due to the adsorption and subsequent desorption of hydroxyls.

Our single crystal study of the reductive desorption of thiols provides new insights into the origin of the differences observed between the thiols deposited on polycrystalline gold samples and on highly ordered gold evaporated on mica. It has been reported that thiols on polycrystalline gold containing high-order crystalline facets are reductively desorbed at more negative potentials than thiols deposited on gold/mica which are formed mainly of Au(111) domains.[18] It is clear from our results on Au(111) and Au(110) (see Figures 5 and 7) that these differences are at least partially related to the pzc of the different crystalline domains present on these substrates. Furthermore, our observation of a reductive desorption of nonanethiols separated from the hydrogen evolution current in neutral solution was only possible on the Au(111) surface. We believe that this is because Au(111) has the most positive pzc of the low-index single crystal surfaces[51] and therefore the thiols are reductively desorbed at less negative potentials. The reductive desorption of nonanethiols from a Au(110) crystal in neutral solution is superposed with the hydrogen evolution current because the thiols are reductively removed at more negative potentials than on Au(111). The superposition of these two reductive processes has prevented the study of the effect of the pH on the reductive desorption of thiols from Au(110). This result suggests that the similar observation of a superposition of the reductive desorption of the thiols and the hydrogen evolution current in neutral or acidic solution reported in many studies[18,20−23,25] using polycrystalline gold is at least partly due to the presence of high index gold domains. Evidently the quality of the thiol monolayer also plays a role in the amount of hydrogen evolution current observed. If a poor thiol layer is formed, a significant hydrogen evolution current will be seen.

In summary, the results for the reductive desorption at the Au(111) single crystal demonstrate that the nonanethiols form a compact monolayer, with the electrochemical data being consistent with adsorption at 3-fold sites giving a $(\sqrt{3}\times\sqrt{3})R30°$ monolayer structure and a coverage of $7.6 \times 10^{-10}$ mol $cm^{-2}$. The reductive desorption process appears to be a one-electron transfer producing a thiolate. The quality of the monolayers on the Au(111) surface is such that the reductive stripping peak is clearly distinguished from any hydrogen evolution current even at neutral pH values. The efficiency of the oxidative redeposition of the reductively desorbed thiols increases as the pH of the electrolyte solution decreases at a slow potential scan rate of 20 mV $s^{-1}$. We suggest that this is linked with the poor solubility of the nonanethiols in solutions of low pH.

In examining the effect of crystal orientation on the behavior of nonanethiols, the first point to note is that the double layer capacitances (estimated from the double layer charging current) are identical on both Au(111) and Au(110) crystals (2.5 $\mu$F $cm^{-2}$) indicating that a compact monolayer can be formed on both surfaces. The thiol coverage estimated from the voltammetric data is $7.5 \times 10^{-10}$ mol $cm^{-2}$. The comparison of the potentials of the reductive current peaks for the Au(111), Au(110), and polycrystalline gold indicates that they are correlated with the potential of zero charge of the uncoated single crystal electrodes.

**Acknowledgment.** The financial support of the Natural Science and Engineering Research Council of Canada is gratefully acknowledged. We thank H. Al-Maznai for the experimental data involving butanethiol.

LA960365Q